UPGRADED METALLURGICAL GRADE SILICON SOLAR CELLS: A DETAILED MATERIAL ANALYSIS

Dietmar Kohler, Bernd Raabe, Stefan Braun, Sven Seren, Giso Hahn
Department of Physics, P.O. Box X916, 78457 Konstanz, Germany
Author for correspondence: dietmar.kohler@uni-konstanz.de, Tel.: +49 7531 883174, Fax: +49 7531 883895

ABSTRACT: Multicrystalline p-type wafers from 100% UMG-Si feedstock were used for two cell processes. The best screen printed solar cells reached an efficiency of 16.2% and fill factors up to 79.7%, while the buried contact cells reached an efficiency of 15.5%, caused by a rather low V_{oc} value of 613 mV. Further analysis of the internal quantum efficiency indicated a low effective diffusion length. Detailed analysis of the lifetime variation within the wafer indicates that the passivation of grain boundaries for the screen printed solar cells is better than for the buried contact solar cells. In a second experiment, screen printed solar cells from different ingot heights were characterized with IV, LBIC (Light Induced Beam Current) and EL (electroluminescence) measurements. Cells from the edge and the centre both showed the similar behaviour. The resistivity increases with ingot height which can be explained by the lower net doping. This leads to a decreasing V_{oc}. The IQE and the j_{sc} increase with ingot height which indicates less recombination. In the highest part of the edge brick we observed patterns in the IQE and series resistance maps, possibly caused by localized impurities or doping variations.
Keywords: Metallurgical-Grade, Buried Contacts, Screen Printing

1 INTRODUCTION

Upgraded metallurgical silicon (UMG-Si) is a cost-effective and energy-efficient silicon material for the production of solar cells. The use of 100% UMG-Si offers access to an additional large amount of silicon produced without the energy consuming purification processes in the Siemens route.

This study includes two experiments. In the first place, wafers from similar height within one ingot brick were processed either with a screen printing or a buried contact process including a buried selective emitter. After each processing step, neighbouring wafers were separated and prepared for lifetime measurements to compare the influences of both processes. Former results showed that high temperature process steps can have a critical influence on the bulk lifetime [1].

For the second experiment we used wafers from two bricks of a second ingot. The positions of the bricks in the centre and on the edge of the ingot allowed a comparison within the ingot. Furthermore the wafers originated from different heights. In this way, also the variation with ingot height could be analysed with means of IV, LBIC and EL measurements.

2 MATERIAL CHARACTERISTICS

In contrast to the complex purification of electronic grade silicon (EG-Si) based on the Siemens route, for UMG-Si the metallurgical-grade silicon is purified without chlorine and crystallized with a special temperature treatment during casting of the ingots.

UMG-Si varies from EG-Si in the following properties which have to be considered for photovoltaic applications. After the above mentioned purification UMG-Si still contains various impurities. Solar cells processed from this material type are mainly influenced by metals and the naturally present dopants boron and phosphor. In contrast to metallic impurities, boron and phosphor cannot be removed efficiently by segregation due to their comparably high segregation coefficients. Resulting from different segregation coefficients, the concentration of the dopants within the ingot leads to an inversion of the polarity type with the lower part being p-type, while the top part of the ingot is n-doped. This part has to be separated and may be processed differently. In between the two parts, the p- and n-type carriers are compensated.

The increasing concentration of the dopants with ingot height is accompanied by a varying bulk resistivity. This leads to a decreasing net charge carrier concentration especially towards the upper part of the ingot where the compensation effect is more pronounced. A further increase in ingot height results in a majority of n-type charge carriers and thus a further increase in the charge carrier concentration. Further on, the mobility of the charge carriers is affected as well [2].

3 CELL PROCESSES

12.5x12.5 cm^2 multicrystalline p-type wafers from 100% UMG-Si feedstock were used for two different solar cell processes. The screen printing (SP) process

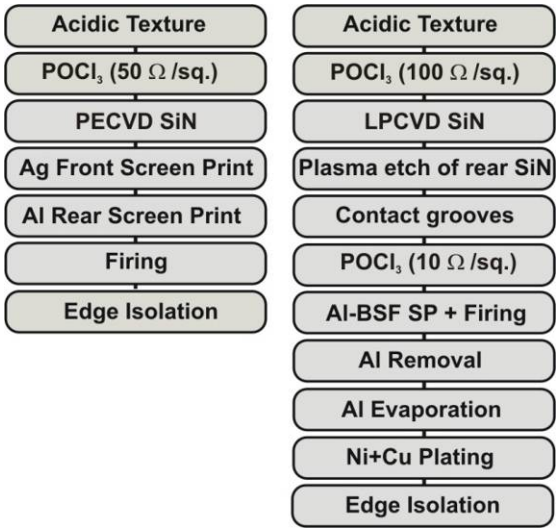

Figure 1: Charts of the screen printed (left) and the buried contact solar cell processes (right).

(Fig. 1 left) reads as follows: The wafers are isotextured with an acidic solution and cleaned. Then a 50 Ω/sq $POCl_3$ diffusion forms the emitter layer. After phosphorus glass removal, hydrogen-rich silicon nitride (SiN_x:H) is deposited by plasma enhanced chemical vapour deposition (PECVD). The metallization is based on screen printing of a Ag front grid and of a full Al rear contact. Finally the cells are fired at an optimized temperature profile and edge isolation is performed by a wafer dicing saw.

The second solar cell process (Fig. 1 right) is a buried contact cell process including a selective emitter structure. After the first $POCl_3$ diffusion resulting in an emitter sheet resistance of 100 Ω/sq, silicon nitride is deposited by low pressure chemical vapour deposition (LPCVD) which provides a denser layer than PECVD SiN_x. A plasma etch is applied to the back which is partly covered with SiN_x. After the SiN_x layer is opened locally by laser grooves where the front grid is to be defined, later a second heavy diffusion results in a lower emitter sheet resistance in the laser opened grooves. For back surface field (BSF) formation, Aluminium is screen printed on the back, fired and afterwards removed by hydrochloric acid etching. Then the rear Al contact is evaporated and is able to sustain the following plating step. After the deposition of a Ni seed and base layer, the Cu plating forms the final front and rear contacts. Edge isolation is done as for the screen printed cells with a wafer dicing saw. For details on the used buried contact process see [3].

The advantages of the buried contact solar cell structure are the selective emitter, resulting in less surface recombination, and smaller finger widths resulting in reduced shading.

4 PROCESS STEP ANALYSIS AND RESULTS

The best screen-printed UMG-Si solar cell reached efficiencies of 16.2% with fill factors up to 79.7%. The buried contact solar cell reached an efficiency of 15.5%, combined with a rather low V_{oc} of 613 mV. By fitting the IV curves increased saturation current densities J_{01} and J_{02} turned out to explain the reduced efficiency compared to the screen printed cells. Further analysis of the internal quantum efficiency (IQE) indicated a low effective diffusion length (see also [3]). In addition, the lifetime was measured by microwave detected photoconductance decay (μ-PCD). After each processing step one wafer was separated, cleaned in a piranha etching solution followed by a diluted hydrofluoric dip. Then the surface was passivated with iodine-ethanol-solution. The results are shown in Fig. 2.

For the BC cell process, the as cut mean lifetime of 26 μs is increased to 39 μs after the first emitter diffusion. This can be explained by phosphorus gettering of impurities. While for the SP process the PECVD SiN_x:H deposition followed by firing further improves the lifetime to 48 μs due to hydrogen passivation of bulk defects, LPCVD carried out at 700°C leads to a decrease to the initial lifetime of 26 μs. This can be explained by a restructuring of defects. The diffusion of the 10 Ω/sq emitter results in an additional gettering and thereby enhances the lifetime to 47 μs. After the firing step of the Aluminium back contact, the lifetime improves even further. The screen printed solar cells show the same improvement, but the indicated integral lifetime is worse due to the low surface passivation quality in the edge parts of the wafer marked in Fig. 2. A detailed analysis of the lifetime variation within the wafer indicates that the passivation of the grain boundaries for the screen printed cells is more effective than for the buried contact cells.

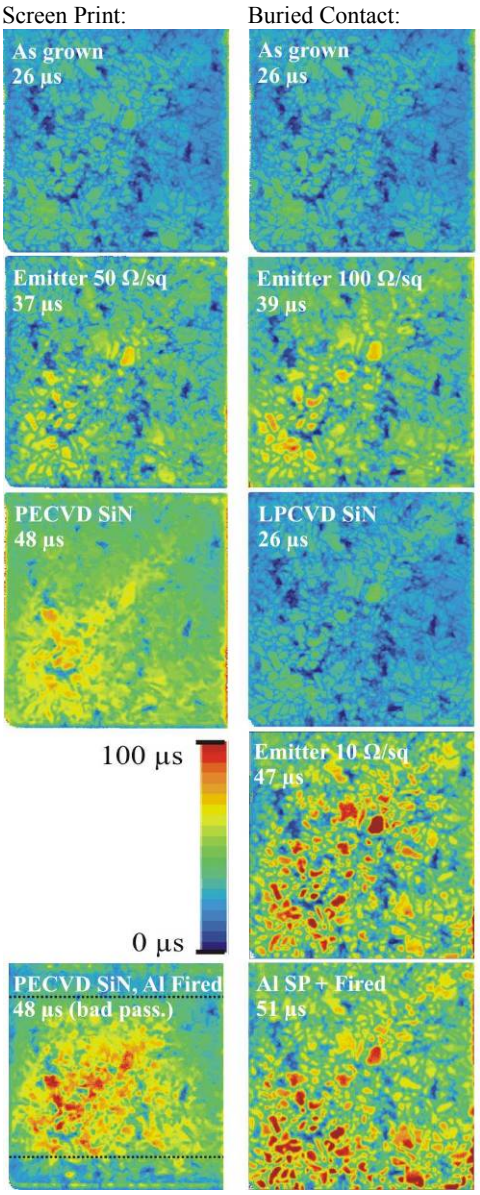

Figure 2: Lifetime maps of neighbouring UMG wafers after different processing steps for the Screen Print (left) and the Buried Contact process (right). The fired Screen Print wafer (bottom left) was poorly passivated in the marked edge parts.

5 INGOT HEIGHT VARIATION

5.1 Experiment

A 100% UMG ingot was cut into 25 bricks. Wafers from the centre brick (M) and an edge brick (F) were processed to solar cells according to the screen printing process as described above. For the centre brick only wafers from the middle region were available. Both bricks showed similar behaviour. The processed cells were characterized with IV, LBIC and EL measurements.

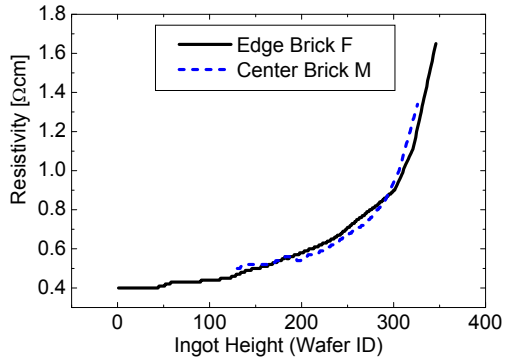

Figure 3: Resistivity against ingot height for two bricks of the same UMG ingot.

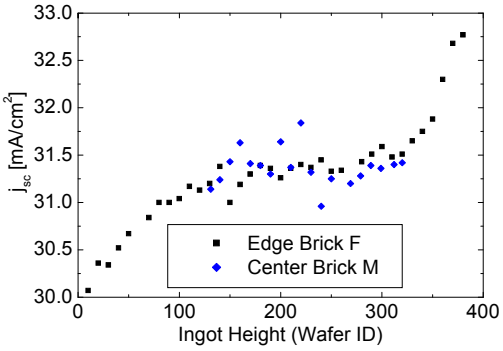

Figure 5: Short current density against ingot height for two bricks of the same UMG ingot.

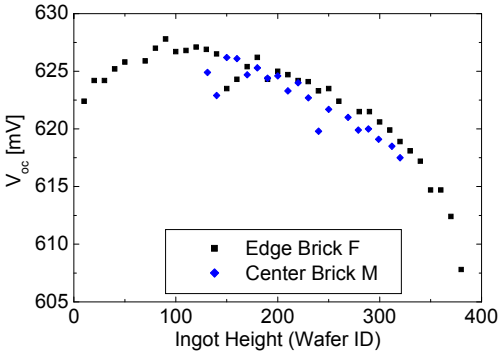

Figure 4: Open circuit voltage against ingot height for two different bricks of the same UMG ingot.

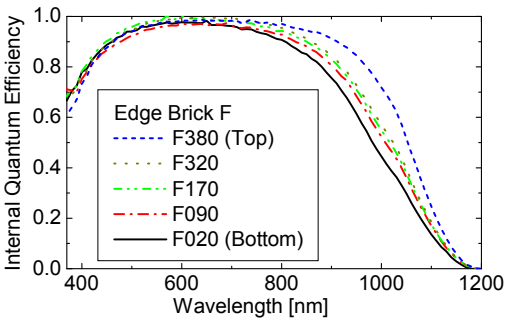

Figure 6: Spectral resolved internal quantum efficiency for cells of different ingot heights.

5.2 Results

The results are shown in Figures 3 to 8. The overall efficiencies are around 15.4%. The fill factors are stable around 79% except for the highest region close to the compensation level. The lower efficiencies in comparison to the above mentioned results are due to the different ingot. Reference cells from the first ingot processed in the same batch reached the same efficiencies of 16% as their neighbouring wafers used for the experiment described in section 4. The differences are caused by both j_{sc} and V_{oc}.

The resistivity of both bricks against ingot height is plotted in Fig. 3. It shows the commonly known height dependence. This is a result of the different segregation coefficients of boron and phosphorus which lead to a decreasing net doping with ingot height and thus less free charge carriers [4].

The open circuit voltage V_{oc} (Fig. 4) increases in the bottom part of the ingot from 622 to 628 mV as a result of the increasing material quality with increasing distance to the crucible walls. From the middle of the ingot towards the type-inversion region, the voltage starts to decrease from its maximum value. This is caused by the increasing resistivity which means a decreasing net doping.

Fig. 5 shows that the short current density j_{sc} strongly increases in the bottom area from 30.1 mA/cm^2 to a plateau at 31.4 mA/cm^2. This is due to impurities in the bottom region which diffused from the crucible into the ingot, resulting in enhanced recombination in this range. In the middle height of the ingot, j_{sc} shows only a small increase, whereas in the top part j_{sc} finally increases up to 32.8 mA/cm^2. This can be explained by the lower net doping leading to less recombination. This development is supported by the internal quantum efficiency (Fig. 6) which reveals a strong increase with ingot height in the longer wavelength regime as a result of an increasing diffusion length. One explanation for the lower net doping or net boron concentration could be the recently proposed possibility of B-P pairs [5].

Caused by the increase of both j_{sc} and V_{oc}, the efficiency also increases in the bottom part to around 15.4% and then remains rather constant.

5.2 Electroluminescence measurements

The EL images in Fig. 7 show the spatially resolved intensity of photo-electrons per second which are proportional to the emitted photons.

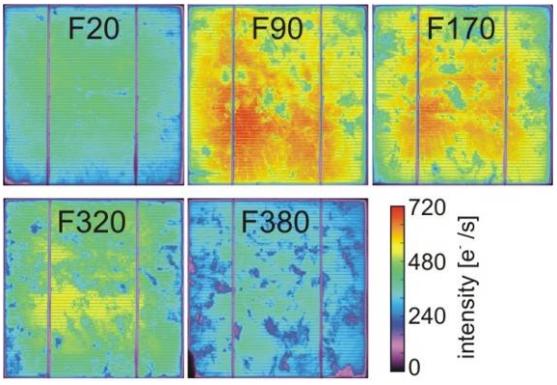

Figure 7: Electroluminescence maps of solar cells from different ingot heights of the edge brick F.

The same trend as observed for the open circuit voltages of the solar cells can be seen. This correlation is consistent with the fact that V_{oc} is also related to the measured difference in the quasi Fermi levels.

These results are in line with the well-known relation that the diffusion voltage is proportional to $\ln(N_A)$, the logarithm of the acceptor concentration in the bulk [6]. The net base doping decreases with ingot height, and so does V_{oc}.

5.3 Curved Patterns

Patterns formed like segments of circles were observed on two wafers from the edge brick just below the compensation height in spatial resolved measurements of the internal quantum efficiency (left in Fig. 8). The same structures are detected in the series resistance mapping using voltage differences at different external currents (right in Fig. 8). Both images indicate that the sectors could be part of rings formed around the centre caused by inhomogeneous crystallization or impurity concentrations in the top end of the p-type ingot part.

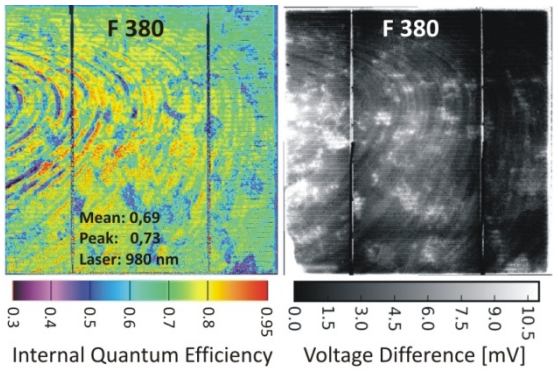

Figure 8: Curved patterns in a solar cell from the ingot part right below the compensation level, observed in LBIC (left) and EL series resistance maps (right).

6 SUMMARY

The use of p-type UMG-Si within a screen printing process resulted in an efficiency of 16.2% with an excellent FF of 79.4%. A main result within this work is the applicability of 100% UMG-Si for an advanced buried contact process which includes different high temperature steps (two emitter diffusions and LPCVD SiN_x deposition) and no hydrogenation of bulk defects. For the buried contact process, an efficiency of 15.5% was reached. Lifetime measurements showed the beneficial effect of a hydrogenation of bulk defects for a SP process (PECVD SiN_x:H). If an effective hydrogenation could be implemented in the BC process as well, the lifetime is expected to increase further and in combination with the beneficial gettering effect of the second emitter diffusion even higher efficiencies are expected.

In a second experiment, variations of material parameters against ingot height within the p-type part were investigated. The solar cells from the centre and the edge brick showed the same behaviour which indicates homogeneous properties of the ingot at the same height. The lower efficiencies compared to the first experiment of about 15.4% with good fill factors of 79% can be explained by using wafers from a different ingot, as another feedstock silicon material was used in this ingot. V_{oc} increases in the lower part of the ingot from 622 to 628 mV as a result of the increasing material quality. Above, the open circuit voltage decreases due to the decreasing net doping. Electroluminescence measurements supported the V_{oc} behaviour.

In the highest part of the available p-type edge brick, spatially resolved measurements of the IQE and the series resistance showed patterns, possibly caused by impurities in combination with the crystallisation conditions.

To investigate this new material in detail, electronic transport mechanisms as Hall mobility will be measured. For detailed studies on reverse current behaviour, measurements of breakdown voltage will be performed.

ACKNOWLEDGEMENTS

The financial support from the BMU project 0325079 is gratefully acknowledged in particular for a part of the sample characterization.

The authors would like to thank S. Ohl, B. Rettenmaier, L. Rothengaß, A. Müller and J. Ruck for their steady support during cell process and D. Kiliani for the EL setup.

REFERENCES

[1] B. Raabe, K. Peter, E. Enabakk, G. Hahn, *"Minority carrier lifetime monitoring in a buried contact solar cell process using mc-Si"*, Proc. 23th EU PVSEC, 1564-1567, 2008

[2] D. Macdonald, F. Rougieux, A. Cuevas, B. Lim, J. Schmidt, M. Di Sabatino, and L. J. Geerligs, *"Light-induced boron-oxygen defect generation in compensated p-type Czochralski silicon"*, J. Appl. Phys. 105, 093704, 2009

[3] S. Braun, B. Raabe, D. Kohler, S. Seren, G. Hahn, *"Comparison of Buried Contact- and Screen Printed 100% UMG Solar Cells Resulting in 16.2% Efficiency"*, 24th EU PVSEC, 2009

[4] J. Kraiem, R. Einhaus, F. Lissalde, S. Dubois, N. Enjalbert, B. Drevet, F. Servant, D. Camel, "*Innovative Crystallisation of Multi-Crystalline Silicon Ingots from different types of Silicon Feedstock"*, Proc. 23th EU PVSEC, 1071-1074, 2008

[5] R. Kopecek, J. Arumughan, K. Peter, E. A. Good, J. Libal, M. Acciarri and S. Binetti, *"Crystalline Si Solar Cells from Compensated Material: Behaviour of Light Induced Degradation"*, Proc. 23th EU-PVSEC, 1855-1858, 2008

[6] A. Goetzberger, B. Voß, J. Knobloch, *"Crystalline Silicon Solar Cells"*,1998, Wiley John + Sons